

## Structure of Binary Liquid Mixtures. II. Resistivity of Alloys and the Ion-Ion Interaction\*

N. W. ASHCROFT AND DAVID C. LANGRETH†

Laboratory of Atomic and Solid State Physics, Cornell University, Ithaca, New York

(Received 17 February 1967)

We have applied the analytic partial structure factors  $S_{ij}(K)$  developed in an earlier work to a study of the resistivity of binary alloys. We find the substitutional model to hold reasonably well, provided that it is modified to incorporate the volume dependence of the pseudopotentials. Deviation from this model can be accounted for by changing the hard-sphere ratio  $\alpha$  [used in obtaining  $S_{ij}(K)$ ] from unity. Such a deviation is non-negligible in Na-K, for example, and is obtained by a calculation of the ion-ion interaction in the alloys. This interaction has been calculated for a number of other alloys as well. Some discussion of the Hg amalgams is also given.

### I. INTRODUCTION

RECENTLY Faber and Ziman<sup>1</sup> have pointed out that whereas the resistivity of solid binary alloys follow Nordheim's and Linde's rules fairly well, their liquid counterparts exhibit little regularity. This anomalous behavior arises from deviations from the simplest possible *substitutional model* in which the alloy is assumed to (i) possess a single structure factor for the ionic configurations (no distinction between species) and (ii) show no variation in atomic volume as the concentration is changed. We find here that most of the concentration dependence of the resistivity arises from a failure of assumption (ii) above, and is easily calculated using a *modified substitutional model*, with simple model volume-dependent pseudopotentials. Finally, in cases where the resistivity is particularly sensitive to the failure of assumption (i), as in alloys of monovalent metals, the deviations (dilatation effects) are straightforwardly included in a more or less first-principles calculation. In Sec. II we outline the modifications of the simple formula for resistivity required by the use of the partial structure factors<sup>2</sup>  $S_{ij}$ , and describe how the  $S_{ij}$  are obtained. In Sec. III we calculate the interionic potential for a number of metals in order to determine the parameters which enter the equation for  $S_{ij}$ . Finally, in Sec. IV we present the results of the resistivity calculations for various liquid alloys including Hg amalgams, and these results are discussed in Sec. V.

### II. FORMULATION OF THE RESISTIVITY FOR BINARY ALLOYS

For a pure liquid metal of valence  $Z$  the simple result for the resistivity of a liquid as first derived by

Ziman<sup>3</sup> may be written

$$\frac{4\pi^3\hbar}{e^2k_F}Z\int_0^1 y^3S(y)V^2(y)dy, \quad (1)$$

where  $V(y)$  is the electron-ion pseudopotential in units of  $\frac{2}{3}E_F$  and  $y$  is the wave-number variable expressed in units of  $2k_F$ .  $S(y)$  is the structure factor for the liquid metal. Although (1) is based on the Born approximation, the results it yields are in remarkably good over-all agreement with experiment for a number of metals, particularly when  $V(y)$  is known from independent means, as for example, when it is determined from Fermi-surface data relating to the solid metals. In a few cases (e.g., the alkali metals) a detailed test of (1) is difficult because of experimental difficulties involved in an accurate determination of the structure factor. This difficulty was partly overcome<sup>4</sup> through the use of a model structure factor which was found to give equally good results in cases (e.g., the polyvalent metals) where more detailed information on  $V(y)$  was available. The model  $S(y)$  was taken from the hard-sphere solution of the Percus-Yevick equation for the radial distribution function in a classical fluid. It was found by Ashcroft and Lekner<sup>4</sup> (AL) that the  $S(y)$  derived in this way gave very good agreement with the x-ray and neutron-scattering data around the first peak. This model structure factor is a function of a single parameter, namely the effective hard-sphere diameter  $\sigma$  for the ion-ion interaction in the liquid. The appropriate  $\sigma$ 's were determined by matching the theoretical solutions to the principal diffraction peak heights. The packing fractions  $\eta$  determined subsequently were found to be near 0.45 for most metals immediately above their melting points. This is close to the observed hard-sphere phase transition as found in the molecular dynamics calculation of Wainwright and Alder.<sup>5</sup> We also note that the relation  $\eta = \text{constant}$  at the melting point is a statement of Lindeman's melting

\* Work supported by the Advanced Research Projects Agency, Report No. 639, through the Materials Science Center at Cornell University, Ithaca, New York.

† Permanent Address: Department of Physics, Rutgers, The State University, New Brunswick, New Jersey.

<sup>1</sup> T. E. Faber and J. M. Ziman, *Phil. Mag.* **11**, 153 (1965).

<sup>2</sup> N. W. Ashcroft and D. C. Langreth, *Phys. Rev.* **156**, 685 (1967), hereafter referred to as I.

<sup>3</sup> J. M. Ziman, *Phil. Mag.* **6**, 1013 (1961).

<sup>4</sup> N. W. Ashcroft and J. Lekner, *Phys. Rev.* **145**, 83 (1966), hereafter referred to as AL.

<sup>5</sup> T. Wainwright and B. Alder, *Nuovo Cimento Suppl.* **9**, 116 (1958).

law<sup>6</sup> viewed from the liquid side of the phase transition. To see this we use the Ornstein-Zernike relation which when combined with the above relation, states that

$$nkT\chi = \text{constant}$$

at the melting temperature. The compressibility  $\chi$  may easily be eliminated in favor of the sound velocity and hence the Debye temperature, so that Lindeman's formula results. The above result is of course independent of the Percus-Yevick approximation.

It is natural to extend these simple ideas to a treatment appropriate to a binary alloy. The modifications are straightforward. The resistivity of a binary alloy in the same approximation may be written as

$$\frac{4\pi^3\hbar}{e^2k_F} Z^* \int_0^1 dy y^3 \{ xV_2^2(y)S_{22}(y) + 2[x(1-x)]^{1/2} \times V_2(y)V_1(y)S_{12}(y) + (1-x)V_1^2(y)S_{11}(y) \}. \quad (2)$$

Here the  $V_i(y)$  are the interactions of an electron with ions of species  $i$  ( $i=1, 2$ ) immersed in the same screening cloud of electrons.  $Z^*$  is an effective valence determined from the ratio of the electron density to the ion density, and  $x$  is the concentration of species 2. For the definition of  $S_{ij}(y)$ , the partial structure factors for the system, we refer to Eq. (4) of I.

To take a particular binary system over the full range of the concentration parameter ( $0 \leq x \leq 1$ ) requires knowledge of the volume dependence of the electron-ion interaction and correspondingly detailed information concerning the behavior of the  $S_{ij}(y)$ . We discuss these in turn.

### A. Volume-Dependent Pseudopotentials

It has recently been proposed<sup>7</sup> that for discussion of transport and equilibrium properties of metals [i.e., properties involving knowledge of  $V(y)$  for  $0 \leq y \leq 2$ ], the following form of potential is adequate, namely,

$$V(y) = -\lambda^2 \text{cossy} / [y^2 + \lambda^2 f(y)], \quad (3)$$

where  $s = 2k_F R_{\text{core}}$ ,  $\lambda^2 = (\pi a_0 k_F)^{-1}$ , and  $f(y)$  is the Lindhard screening function. The quantity  $R_{\text{core}}$  represents an effective core radius outside of which the unscreened electron-ion interaction is Coulomb-like, and inside of which the potential appropriate to a pseudo-plane-wave approximation is virtually zero. This potential accounts for the cancellation in the core region inherent in the case of pseudo plane waves for the electron wave functions. The  $R_{\text{core}}$ , as determined from Fermi-surface data, is found to agree well with the usual ionic radii. This may be anticipated from the range of cancellation

<sup>6</sup> See, for example, David Pines, *Elementary Excitations in Solids* (W. A. Benjamin, Inc., New York, 1963), p. 37.

<sup>7</sup> N. W. Ashcroft, *Phys. Letters* **23**, 48 (1966); N. W. Ashcroft (to be published). This model potential was used rather successfully by N. W. Ashcroft and D. C. Langreth, *Phys. Rev.* (to be published) to calculate the binding energies and compressibilities of simple metals.

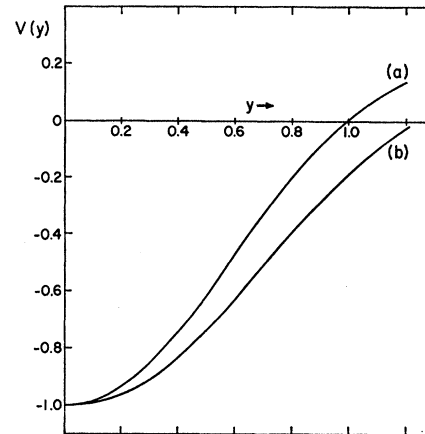


FIG. 1. The pseudopotential form factor  $V(y)$  of a Na ion in (a) an electron density appropriate to pure Na and (b) an electron density appropriate to pure K. The resistivity is most sensitive to the value of  $V(y)$  in the region  $y \sim 1$ .

expected. If we assume the cancellation to be an inherent property of the ion core whose effectiveness is governed by the extent and detailed nature of the core states, then, provided the cores are well removed in energy from the band states, we expect  $R_{\text{core}}$  to be only weakly dependent on electron density. The latter has been roughly demonstrated in the extreme case where the potential leading to (3) is treated as an isolated atomic potential and used to bind the valence electrons. The ionization energies define an effective core radius in good agreement with  $R_{\text{core}}$  appropriate to the metallic state for most of the simple metals. The agreement is less good for metals in which the core states are poorly separated in energy from the band states and this leads to our proviso above.

Thus, for alloys comprised of ions with tightly bound cores we use

$$V_i(y) = -\frac{\lambda^2 \text{coss}_i y}{y^2 + \lambda^2 f(y)} \frac{Z_i}{Z^*}, \quad (4)$$

with  $s_i = 2k_F R_{\text{core}}^i$ . The Fermi momentum  $k_F$  is common to both potentials. As an example we show in Fig. 1 the pseudopotential of a sodium ion in (a) an electron density appropriate to pure sodium and (b) an electron density appropriate to pure potassium (i.e., a single sodium ion in a potassium host). When viewed in terms of the integrals in both (1) and (5), it is apparent that density changes in the potential can be quite important. The simple form (4) cannot of course be correct for alloys in which the electron concentration is depleted by chemical bonding (as indicated by an exothermic reaction). This automatically excludes from the present consideration a large group of the mercury amalgams.

### B. Structure Factors for Binary Alloys

As mentioned in the Introduction, we propose to use for the  $S_{ij}(y)$  the hard-sphere momentum-space

solutions of the Percus-Yevick (PY) equation appropriate to binary mixtures.<sup>8</sup> These are set out in detail in I, and since the solutions are lengthy we do not repeat them here but simply refer to the essential equations as required. In terms of the Ornstein-Zernike correlation functions  $C_{ij}(y)$  we may write

$$\begin{aligned} S_{11}(y) &= [1 - n_2 C_{22}(y)] / D(y), \\ S_{22}(y) &= [1 - n_1 C_{11}(y)] / D(y), \end{aligned} \quad (5)$$

and

$$S_{12}(y) = (n_1 n_2)^{1/2} C_{12}(y) / D(y),$$

where

$$D(y) = [1 - n_1 C_{11}(y)][1 - n_2 C_{22}(y)] - n_1 n_2 C_{12}^2(y),$$

and where the  $n_i$  are number densities of the  $i$ th component. For a mixture of hard spheres whose diameters are in the ratio  $\alpha$  ( $\alpha \leq 1$  by choice), and whose concentration is governed by a parameter  $x$  for the larger component, the PY approximation leads to Eqs. (B1) and (B2) of I for the  $C_{ij}(y)$ . One further parameter, the total packing fraction  $\eta$ , completes the description.

A discussion of the determination of  $\eta$  and  $\alpha$  as functions of concentration will be deferred until Sec. III. The case  $\alpha = 1$  deserves special mention, however, because it corresponds to the modified substitutional model which takes full account of the change in *mean* atomic volume. We find that for alloys of polyvalent metals this atomic volume change is the only important effect, and that even for monovalent alloys, it is the dominant effect. From (2) and (5), in which the  $C_{ij}(y)$  are now all equal, we find immediately that the resistivity is given by

$$\frac{4\pi^3 \hbar}{e^2 k_F} Z^* \int_0^1 dy y^3 \{ x V_2^2(y) S(y) + x(1-x) [V_1(y) - V_2(y)]^2 \times [1 - S(y)] + (1-x) V_1^2(y) S(y) \}, \quad (6)$$

where

$$S(y) = [1 - nc(y)]^{-1}.$$

### III. THE ION-ION POTENTIAL: THE VALUES OF $\eta$ AND $\alpha$

Here we calculate the actual Born-Oppenheimer potential acting between two ions in the liquid. We do this both as a justification for the hard-sphere model of a liquid metal, and as a method for determining the parameters  $\eta$  and  $\alpha$ .

Before proceeding, however, we mention that for pure metals just above their melting points AL found that  $\eta = 0.45$  almost universally. We similarly expect here that physically interesting values of  $\eta$  will be close to this. We also would intuitively expect the ratio of hard-sphere diameters to be close to unity. Correspondingly, in alloys of polyvalent metals where the resistivity is

<sup>8</sup> J. L. Lebowitz, Phys. Rev. **133**, A895 (1964).

not extremely sensitive to the structure we set  $\eta = \text{constant}$ ,  $\alpha = 1$  for a number of cases (as indicated in the figures) for the whole range of concentrations.

For the alkalis, however, this approximation is quantitatively inadequate. Hence, we set out to calculate the ion-ion potential, from which  $\eta$  and  $\alpha$  may be determined directly. Within the pseudopotential scheme, lowest-order perturbation theory has been at least moderately successful in predicting correctly a number of electronic properties of simple metals. It is natural then to anticipate that it will predict reasonably good ion-ion potentials as well. In such an approximation, the ion-ion interaction is a central, two-body potential given (in units of  $\frac{2}{3}$  the Fermi energy of the alloy) by

$$\begin{aligned} \phi_{ij}(\rho) &= [3(Z^*)^2/\pi] \int d^3y e^{i\rho \cdot y} V_i(y) V_j(y) (y^2/\lambda^2) \\ &\times [\epsilon^{-1}(y) - 1] + 6\pi\lambda^2 Z_i Z_j / \rho, \end{aligned} \quad (7)$$

where  $V_i(y)$  is the bare (unscreened) pseudopotential form factor of species  $i$ ,  $\epsilon(y)$  is the dielectric function of the *interacting* electron gas, and  $\rho$  is  $2k_F$  times the distance between ions. The last term in (7) is the bare ion-ion interaction which is assumed Coulombic. The validity of this latter approximation will be verified later, when we find (as found empirically by AL) that the potential (7) is sufficiently repulsive to prevent the ionic cores from overlapping.

In evaluating (7), it is extremely important that accurate values of  $\epsilon(y)$  be used. The random-phase approximation (RPA), although sufficiently accurate to describe the screening of the potentials<sup>9</sup> in (1), (2), and (6), is inadequate here because the combination  $\epsilon^{-1} - 1$  is particularly sensitive to errors in the polarizability. Now Hubbard<sup>10</sup> has shown that a number of important terms in the perturbation theory for the polarization part may be summed approximately by writing

$$\epsilon(y) = 1 + \frac{\lambda^2}{y^2} \frac{f(y)}{1 - \lambda^2 f(y)/(2y^2 + g)}, \quad (8)$$

where  $g$  is a function of density alone. Several different forms of  $g$  have been proposed in the literature.<sup>10-12</sup> However, for the values of ionic separation of interest (near the "hard-sphere diameter"), the integral (7) is dominated by fairly small  $y$ , so it is compelling to choose

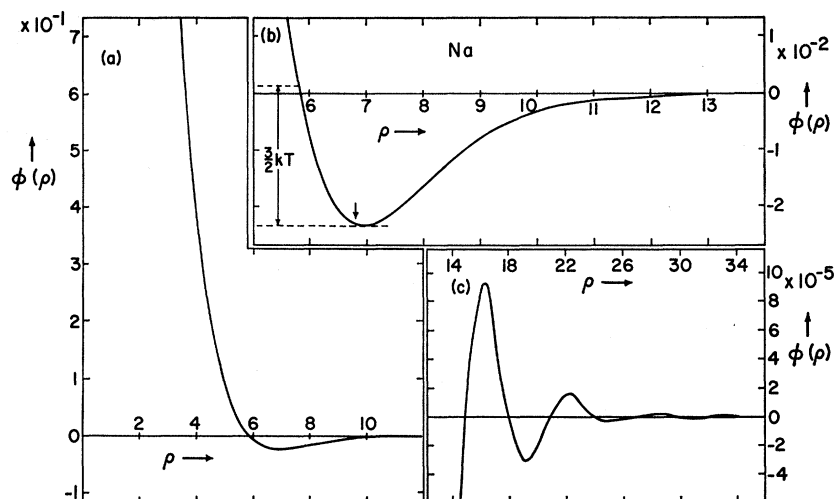
<sup>9</sup> In addition to corrections to Lindhard screening, the potentials in (1), (2), and (6) should contain a vertex correction, which accounts for exchange scattering with electrons in the screening cloud. Both corrections are relatively unimportant because the integrands are weighted at fairly large momentum transfers, where Coulomb effects are small. The remnant errors are adequately absorbed into our parametrization scheme.

<sup>10</sup> J. Hubbard, Proc. Roy. Soc. (London) **A243**, 336 (1957).

<sup>11</sup> L. M. Falicov and V. Heine, Advan. Phys. **10**, 57 (1961).

<sup>12</sup> D. J. W. Geldart and S. H. Vosko, Can. J. Phys. **44**, 2137 (1966).

FIG. 2. The calculated ion-ion interaction in pure Na. The hard-core nature of this interaction is demonstrated in (a). In (b) we show the region around the first minimum;  $\frac{3}{2}kT$  (at 100°C) is shown on the same scale; this temperature corresponds to a hard-sphere diameter  $2k_F\sigma=5.8$ , which compares favorably with the value of 5.9 found by AL; the arrow shows the nearest-neighbor distance in solid Na. The continuation of (a) is scaled by a factor  $5 \times 10^3$  in (c) in order to show the Friedel oscillations.



$g$  such that the identity<sup>13</sup>

$$\lim_{y \rightarrow 0} y^2 \epsilon(y) = \lambda^2 K / K_0 \quad (9)$$

is satisfied. Here  $K/K_0$  is the compressibility of the interacting electron gas measured in units of the noninteracting electron-gas compressibility and is known quite accurately. For its evaluation we have used the Nozières-Pines interpolation<sup>13</sup> formula,

$$K/K_0 \approx (1 - \lambda^2 - 0.158\lambda^4)^{-1}. \quad (10)$$

Actually, for the lower-density metals, it is not very relevant whether (10) be quantitatively accurate; what is important is that  $K/K_0$  is sufficiently large that  $1/\epsilon - 1 \approx -1$  over most of the important region of integration.

In Fig. 2 we show the results for the potential  $\phi(\rho)$  between two Na ions immersed in an electron gas of density appropriate to that of liquid Na just above its melting point. We expect our potential to be the most accurate in the region shown in Fig. 2(b). Figure 2(a) is included to show the "hard-sphere" nature of the potential, and Fig. 2(c) to show that the Friedel oscillations appear as they should.

We now use this potential to determine an effective hard-sphere diameter  $\sigma$  (or packing fraction  $\eta$ ), for use in the PY equation. Presumably, this diameter is determined approximately by

$$\phi(2k_F\sigma) - \phi_{\min} \approx \frac{3}{2}kT / \frac{2}{3}E_f, \quad (11)$$

where  $\phi_{\min}$  is the value of  $\phi$  at its minimum. Application of (11) to the curve of Fig. 2(b) yields  $\eta \equiv (2k_F\sigma)^3 / 144\pi Z = 0.44$  at 100°C. This is in good agreement with the value of  $\eta = 0.45$  found by AL. From the slope of the potential at  $\rho = 2k_F\sigma$ , the quantity  $d\eta/dT$  may also be determined. We find for Na at 100°C that  $(d\eta/dT) = -3.0 \times 10^{-4}/^\circ\text{C}$ , which is in excellent agreement with

<sup>13</sup> For example, see David Pines and P. Nozières, *The Theory of Quantum Liquids* (W. A. Benjamin, Inc., New York, 1966), Vol. I.

the value of  $-3.05 \times 10^{-4}/^\circ\text{C}$  implied by the work of AL. In view of these results, we feel that we can extend the results to Na-K alloys with some confidence. We also mention that in the region of the hard-sphere diameter, our Na potential agrees very closely with the one determined semiempirically by Johnson, Hutchinson, and March<sup>14</sup> using the Percus-Yevick theory.

Our results<sup>15</sup> are displayed in Figs. 3-6. Finally, as indicated in Fig. 2, the nearest-neighbor distance in the solid is close to the minimum of the ion-ion interaction. Figure 3 shows the Na-Na, Na-K, and K-K interactions,

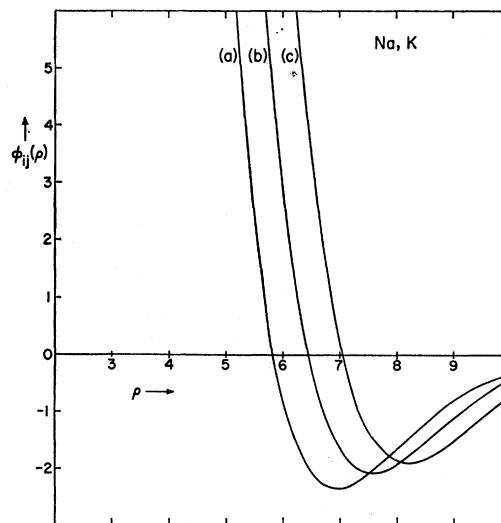


FIG. 3. The calculated interaction  $\phi_{ij}(\rho)$  between (a) two Na ions, (b) a Na ion and a K ion, and (c) two K ions immersed in an electron gas of density appropriate to pure liquid Na at 100°C.

<sup>14</sup> M. D. Johnson, P. Hutchinson, and N. H. March, *Proc. Roy. Soc. (London)* **A282**, 283 (1964). On the other hand, the amplitude of the oscillatory part of their potential is considerably larger than the amplitude we find.

<sup>15</sup> In determining the actual density of the alloys we have made a linear interpolation in volume. Thus,  $\Omega_{\text{alloy}} = (1-x)\Omega_1 + x\Omega_2$ , where  $\Omega$  is the atomic volume involved. This seems to be well in accord with the available experimental data.

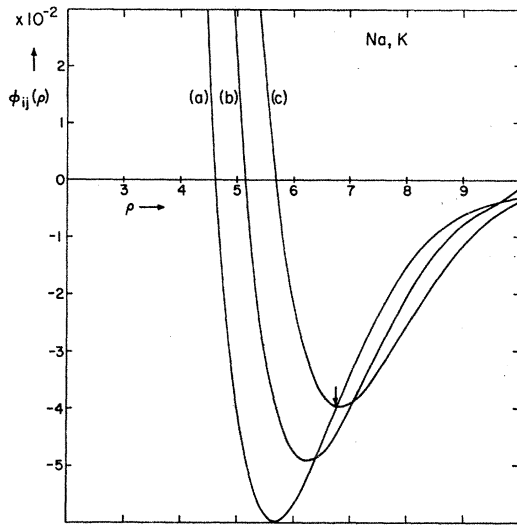


FIG. 4. The calculated interaction between (a) two Na ions, (b) a Na and a K ion, and (c) two K ions immersed in an electron gas of density appropriate to pure liquid K at 100°C. The arrow marks the nearest-neighbor distance in solid K.

when these ions are immersed in an electron gas of density appropriate to that of pure Na. Figure 4 shows these interactions for electron-gas density appropriate to that of pure K. Figures 5 and 6 show similar results

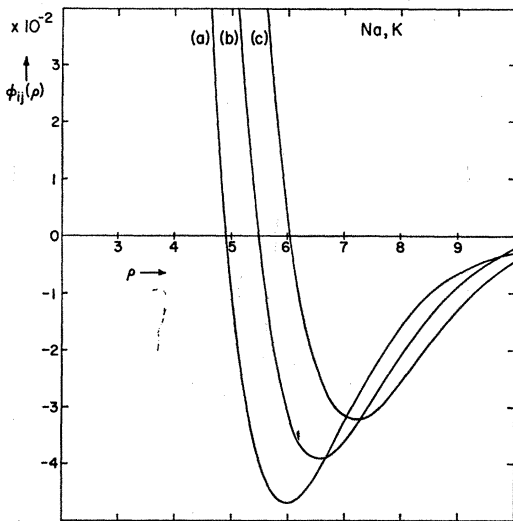


FIG. 5. The calculated interaction between (a) two Na ions, (b) a Na ion and a K ion, and (c) two K ions immersed in an electron gas of density appropriate to 32.4% Na and 67.6% K.

for the electron-gas densities of two different Na-K alloys.

One fact that is clear immediately by inspection of the curves is that

$$\sigma_{\text{Na-K}} \simeq \frac{1}{2}(\sigma_{\text{Na-Na}} + \sigma_{\text{K-K}}). \quad (12)$$

This is fortunate because (12) was implicitly assumed in the derivation of the structure factors which we use.

Next we employ (11) to calculate the hard-sphere diameters. We find for the packing fraction

$$\eta \equiv (\pi/6)[(1-x)\sigma_1^3 + x\sigma_2^3](2k_f)^3 \simeq 0.43 \pm 0.02$$

over the whole range of concentration. The calculation is not sufficiently accurate to predict the detailed variation of  $\eta$  as a function of concentration, but it

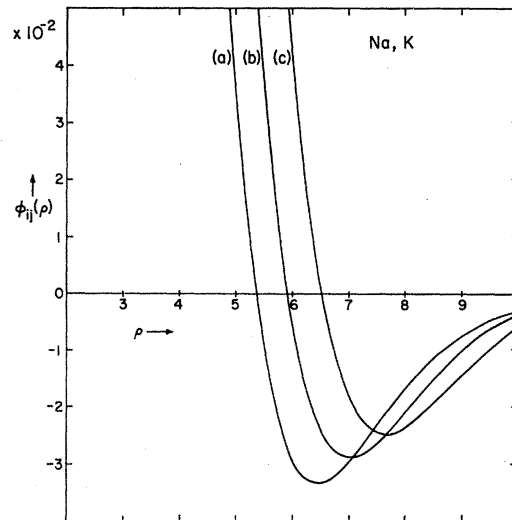


FIG. 6. The calculated interaction between (a) two Na ions, (b) a Na and a K ion, and (c) two K ions immersed in an electron gas of density appropriate to 68.5% Na and 31.5% K.

does serve to verify our earlier speculation that such variation is small. For actual resistivity calculations it will be sufficient to make a linear interpolation between the value appropriate to pure Na and that of pure K (at the temperature involved).

The new result that emerges from our analysis is the value  $\alpha$ , the hard-sphere ratio. We find that

$$\alpha \equiv \sigma_1/\sigma_2 \simeq 0.835 \pm 0.010$$

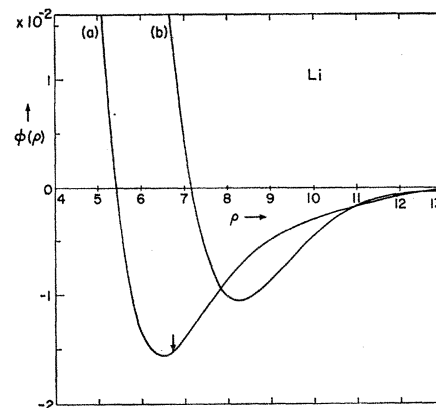


FIG. 7. The calculated interaction between two Li ions immersed in an electron gas of density appropriate liquid Li metal at 200°C. Curve (a) corresponds to  $R_{\text{core}} = 0.56 \text{ \AA}$ ; curve (b) corresponds to  $R_{\text{core}} = 1.06 \text{ \AA}$ . Both values of  $R_{\text{core}}$  yield the correct pure liquid resistivity but only the smaller value gives a reasonable value of both  $2k_f\sigma$  and the ion-ion separation indicated by the arrow.

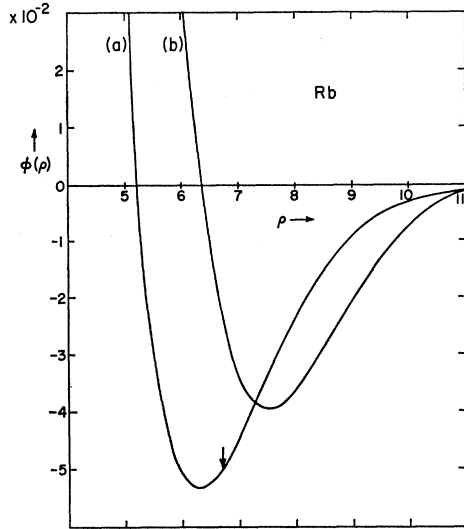


FIG. 8. The calculated interaction between two Rb ions immersed in an electron gas of density appropriate to liquid Rb at 40°C. Curve (a) corresponds to  $R_{\text{core}}=1.12 \text{ \AA}$  while curve (b) corresponds to  $R_{\text{core}}=1.44 \text{ \AA}$ . Both values yield the correct pure-liquid resistivity (see text) but only the smaller value gives a reasonable value for  $2k_{FS}$  and the nearest-neighbor separation indicated by the arrow.

for the whole range of concentration in the Na-K system. As we shall see later, the difference in resistivity predicted for  $\alpha \sim 1$  and  $\alpha \sim 0.8$  is substantial.

Of the remaining alkalis we have computed the ion-ion interactions in Li and Rb and the results are shown in Figs. 7 and 8. For each metal we have used

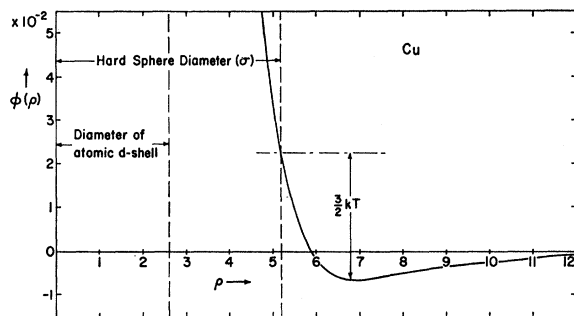


FIG. 9. The calculated interaction between two Cu ions immersed in an "s"-electron gas of density appropriate to liquid Cu at 1200°C.

two core radii (indicated), both of which are consistent with the resistivities of the pure liquid metals. It is evident from the figures that the smaller radius in each case is in good agreement with the observed packing fractions. A similar calculation (Fig. 9) for the monovalent metal Cu has been carried out with an  $R_{\text{core}}=0.43 \text{ \AA}$  which is chosen to fit the resistivity of the pure liquid metal. The significance of the simple free-electron theory as applied to a metal with  $d$  states is discussed in Sec. V.

We have also computed the ion-ion interaction in Hg, Al, and Pb. The  $R_{\text{core}}$  for Hg was again chosen to fit the pure-liquid resistivity: Again two choices are possible with the smaller radius giving the better agreement with the observed packing fraction as shown in Fig. 10. In Al,  $R_{\text{core}}=0.59 \text{ \AA}$  is determined by Fermi-surface studies,<sup>7</sup> and the ion-ion interaction given by

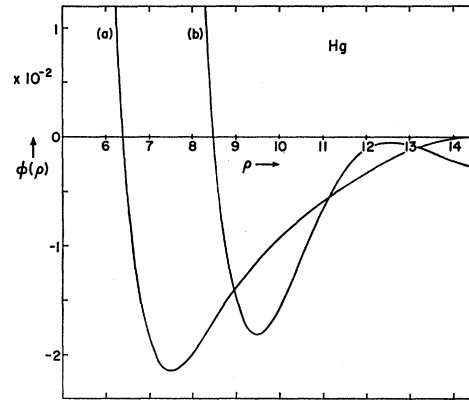


FIG. 10. The calculated interaction between two Hg ions immersed in an "s"-electron gas of density appropriate to liquid Hg at 50°C. Curve (a) corresponds to  $R_{\text{core}}=0.484 \text{ \AA}$ ; curve (b) corresponds to  $R_{\text{core}}=0.860$ . Again, both values yield the correct pure-liquid resistivity (see text) but the smaller value gives the better agreement with  $2k_{FS}$  and the nearest-neighbor distance. As with Cu, the hard-sphere diameter is considerably outside the atomic  $d$ -shell diameter.

Eq. (7) is shown in Fig. 11. Also shown in this figure is the same interaction calculated at the density found in the solid metal. The rather dramatic density dependence of the ion-ion potential (in the region of the next-nearest-neighbor distance) is most pronounced in the high-density metals where Eq. (7) is sensitive to the value of  $\epsilon(y)$ .

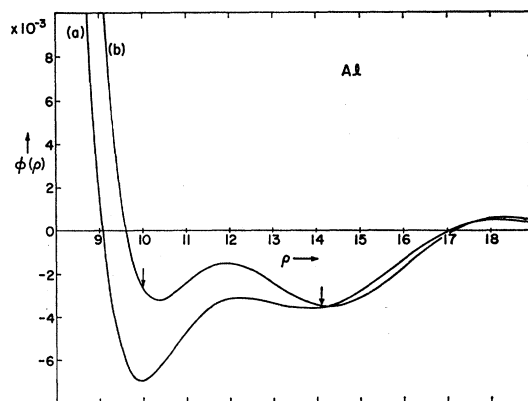


FIG. 11. The calculated interaction between two Al ions immersed in an electron gas of density appropriate to (a) liquid Al at 660°C, and (b) solid Al at room temperature. The arrows show the nearest-neighbor and next-nearest-neighbor distances. The volume dependence of the ion-ion interaction is most pronounced in high-density metals (as above) where Eq. (7) is most sensitive to the value of  $\epsilon$ .

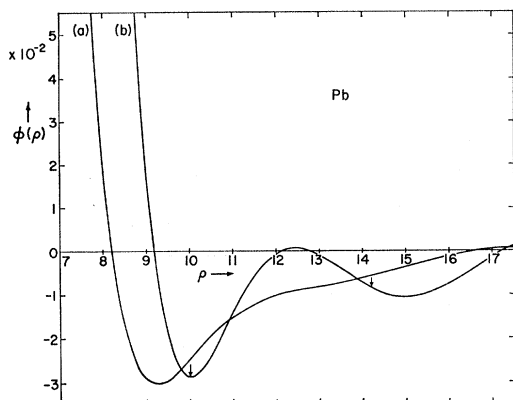


FIG. 12. The calculated interaction between two Pb ions immersed in an electron gas of density appropriate to liquid Pb at 350°C. Curve (a) corresponds to  $R_{\text{core}}=0.59$  Å and curve (b) corresponds to  $R_{\text{core}}=0.78$  Å (see text). The latter gives good values for  $2k_{\text{FS}}$  and also for the nearest-neighbor distance shown by an arrow.

Finally, we show in Fig. 12 the ion-ion interaction in Pb for two values of  $R_{\text{core}}$ . The final choice of  $R_{\text{core}}$  for this metal is discussed in the next section.

#### IV. ELECTRICAL RESISTIVITIES OF BINARY ALLOYS

We turn now to an application of Eq. (2) to a number of alloys, commencing with the Na-K system. Although each component has a resistivity of around  $10 \mu\Omega$  cm just above its melting point, an alloy of equal parts yields a resistivity of about  $40 \mu\Omega$  cm, a substantial increase. For both pure Na and K at 150°C the resistivities have been evaluated with the  $R_{\text{core}}$  given in Table I and  $\eta$  is adjusted to the compressibility as outlined in AL. These were chosen to give the correct resistivities at their melting points with  $\eta=0.456$  and in both cases

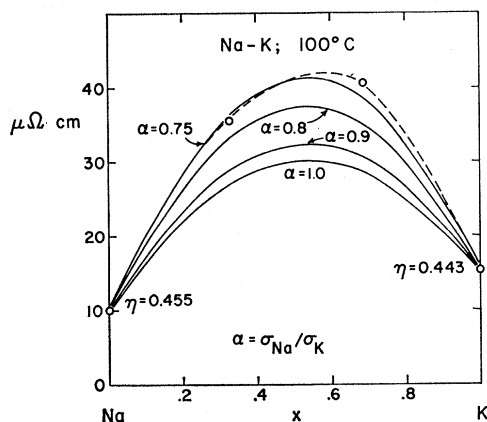


FIG. 13. The calculated resistivity for the Na-K system at 100°C, for several different  $\alpha$  values. The curve for  $\alpha=0.8$  best fits the experimental points on the interpolated dashed curve. These were taken from Ref. 18. For pure Na we use  $\eta=0.455$  and for pure K we use  $\eta=0.443$  (both values are appropriate to 100°C).

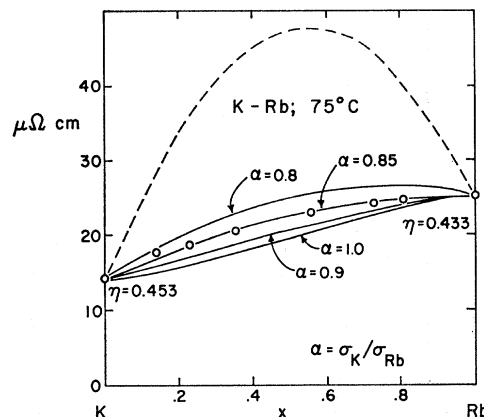


FIG. 14. Calculated resistivity of the K-Rb system at 75°C. The experimental points are taken from Ref. 19. The solid curves correspond to different values of  $\alpha$  for  $R_{\text{core}}(\text{Rb})=1.12$  Å. The dashed curve corresponds to  $R_{\text{core}}(\text{Rb})=1.44$  Å (and  $\alpha=1$ ). For pure K we use  $\eta=0.453$  and for pure Rb we use  $\eta=0.433$  (at 75°C).

$R_{\text{core}}$  is in accord with the Fermi-surface data.<sup>7,16</sup> Throughout the range of concentration, values of  $\eta$  were chosen in two ways: (a) a smooth interpolation between  $x=1$  and  $x=0$  and (b) by using the difference between the working temperature and the liquidus (along which we assume  $\eta=0.456$ ) together with the  $d\eta/dT$  curves for pure K and Na (which are similar) and also assuming a similar variation in the alloy. The difference in the results of the two methods amounts to only  $\sim 2 \mu\Omega$  cm at the most and therefore cannot be considered significant. For the present, we regard the linear interpolation to be sufficiently accurate. A plot of resistivity against  $x$  is given in Fig. 13: The experimental data are taken from Freedman and Robertson<sup>17</sup> and from the *Liquid Metals Handbook*.<sup>18</sup> The four theoretical curves correspond to  $\alpha=1$  (modified substitutional model),  $\alpha=0.9$ ,  $0.8$ , and  $0.75$ . The last is seen to fit the data quite well, and this value of  $\alpha$  is close to that obtained in the previous section.

TABLE I. Core parameters (in angstroms) used to fix the Fourier transform of the electron-ion interaction in the transport region. The values in parentheses are alternative values of  $R_{\text{core}}$  which also reproduce the resistivity of the pure liquid metals but give poor agreement for other properties as discussed in the text.

Metal	$R_{\text{core}}$	Metal	$R_{\text{core}}$
Li	0.560 (1.06)	Hg	0.484 (0.856)
Na	0.880	Zn	0.673
K	1.115	Al	0.590
Rb	1.120 (1.44)	In	0.700 (0.590)
Cu	0.430 (0.93)	Sn	0.686
Ag	0.550 (0.99)	Pb	0.780 (0.59)
Au	0.430 (1.08)	Bi	0.790

<sup>16</sup> M. J. G. Lee, Proc. Roy. Soc. (London) **A295**, 440 (1966).

<sup>17</sup> J. F. Freedman and W. D. Robertson, J. Chem. Phys. **34**, 769 (1961).

<sup>18</sup> *Liquid Metals Handbook* (U. S. Office of Naval Research in Cooperation with the Atomic Energy Commission, Washington, D. C., 1952).

In Fig. 14 we show the results of our calculations on the K-Rb system. The data are taken from Kurnakow and Nikitinsky.<sup>19</sup> The theoretical curves shown correspond to  $R_{\text{core}}=1.44 \text{ \AA}$  (dashed) and  $R_{\text{core}}=1.12 \text{ \AA}$  (full curves). The latter with  $\alpha=0.85$  is seen to be in reasonable agreement with the alloy data, and in particular with the resistivity for pure Rb at  $75^\circ\text{C}$ . We comment on this in the next section.

In Fig. 15 we show the results for the Pb-Sn system at  $500^\circ\text{C}$ . This temperature is reasonably near to the melting points of both metals; and in accordance with the results of Ashcroft and Lekner, we expect a packing fraction of close to 0.45 to be valid throughout the concentration range. The results for the modified substitutional model given in Fig. 15 are in good agreement with the data of Adams and Leach.<sup>20</sup> Table I summarizes the  $R_{\text{core}}$  data used here. No account has been taken here of the contribution to the scattering from spin-orbit terms in the potential.<sup>21</sup> The  $R_{\text{core}}$  for lead is somewhat different from the value which is in accord with the Fermi-surface data for the crystalline solid. This (central) potential leads to poor agreement with the data (cf. also the Hg-Pb system as discussed more fully below).

### Mercury Amalgams

The mercury amalgams are interesting in that apart from Na, K, Rb, and Cs (which show some evidence of chemical bonding) all other metals produce a sharp decrease in resistivity when alloyed in Hg. It is appealing to attempt to explain these results in terms of the model proposed here. There is at the outset a difficulty in that it is by no means apparent that simple free-electron theory is appropriate to Hg. This follows from the experimental observation of the presence of  $d$ -state electrons which have also been predicted in the calcula-

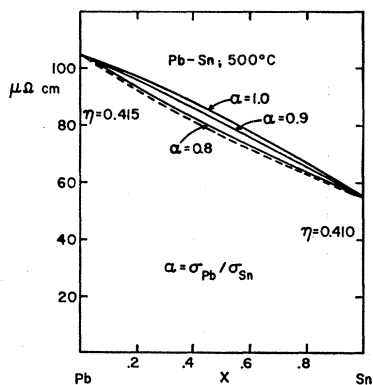


FIG. 15. Calculated resistivity of the Pb-Sn system at  $500^\circ\text{C}$ . The experimental curve (dashed) summarizes the data of Ref. 20. The  $\eta$  values used here are  $\eta=0.410$  for Sn and  $\eta=0.415$  for Pb.

<sup>19</sup> N. S. Kurnakow and A. J. Nikitinsky, *Z. Anorg. Allgem. Chem.* **88**, 151 (1914).

<sup>20</sup> P. D. Adams and J. Leach, *Phys. Rev.* **156**, 178 (1967).

<sup>21</sup> A. O. E. Animalu, *Phil. Mag.* **13**, 53 (1966).

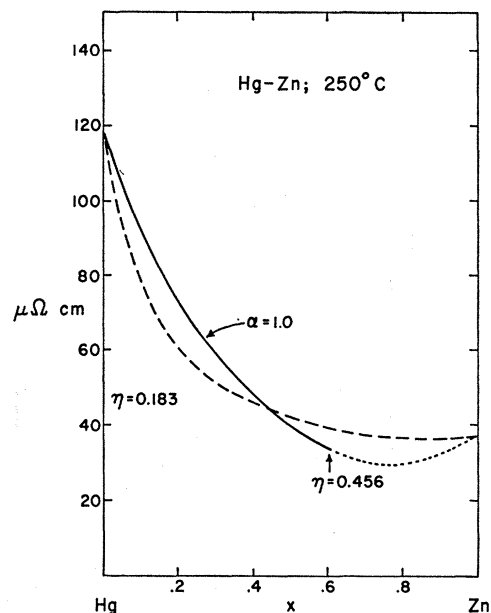


FIG. 16. Calculated resistivity for the Hg-Zn system at  $250^\circ\text{C}$  with  $\alpha=1$ . The dashed experimental curve is taken from Adams and Leach (private communication). The dotted portion of the theoretical curve indicates a solid alloy. The  $\eta$  value for Hg is 0.183 and for Zn is 0.456.

tions of Keeton and Loucks.<sup>22</sup> The  $d$  states are evidently located near the bottom of the  $s$ -electron conduction band. It follows that our criterion for the applicability of Eq. (4) for the electron-ion interaction is not exactly

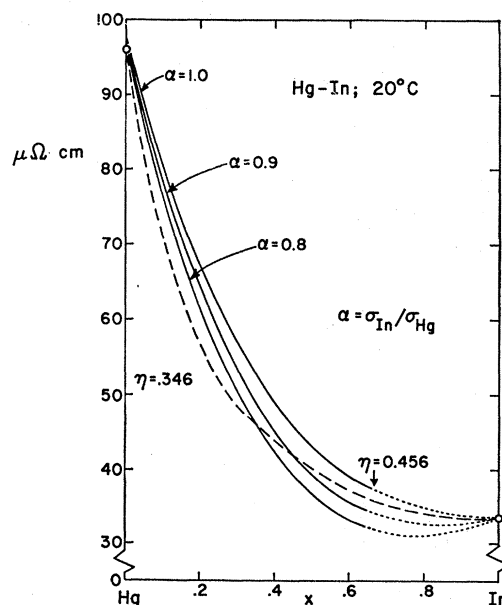


FIG. 17. Calculated resistivity for the Hg-In system at  $20^\circ\text{C}$  for several  $\alpha$  values. The dashed curve summarizes the experimental points of Ref. 25. The  $\eta$  values used are 0.346 for Hg and 0.456 for In. The dotted portions of the curves indicate regions of solid alloy.

<sup>22</sup> S. C. Keeton and T. L. Loucks, *Phys. Rev.* **152**, 548 (1967).

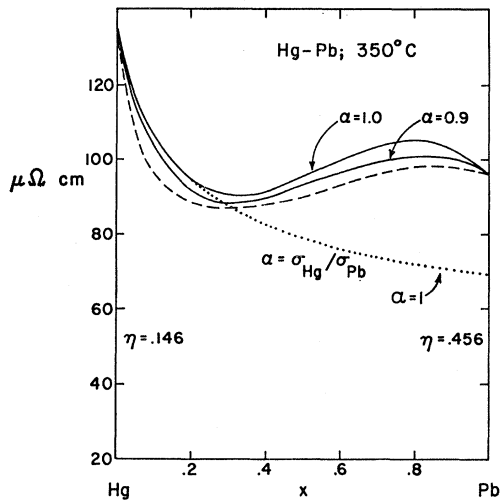


FIG. 18. Calculated resistivity of the Hg-Pb system at 350°C. The solid curves correspond to  $R_{\text{core}}=0.78 \text{ \AA}$  and  $\alpha=1.0$  and  $0.9$ . The dotted curve corresponds to  $\alpha=1$ , but  $R_{\text{core}}=0.59 \text{ \AA}$ . The dashed experimental curve summarizes the data of Adams and Leach [P. D. Adams (private communication)]. The  $\eta$  value for Pb is 0.456, and for Hg is 0.146.

met. As a consequence, we cannot expect the form of the potential to be invariant with changes in electron density. On the other hand, if the  $d$  states are not too close to the Fermi surface (which from Fermi-surface studies appears  $s$ -like<sup>23</sup>), then the changes in this potential may not be too important as regards transport properties, although the energy derivatives of the potential may have a marked effect on, say, the thermopower. It follows that we may use, with some caution, the simple potential and evaluate the parameter  $R_{\text{core}}$  from the resistivity data for the pure metal. At 20°C  $R_{\text{core}}=0.484 \text{ \AA}$ , which compares reasonably well with the radius of the isolated potential required to yield the ionization energy<sup>7</sup> ( $R_s=0.52 \text{ \AA}$ ). An alternative value  $R_{\text{core}}=0.856 \text{ \AA}$  also gives the correct pure-liquid resistivity but is in poor agreement with the temperature dependence and also with the alloying data which we now present. Finally, as shown in Fig. 10, the latter value gives an ion-ion potential which corresponds to the value of  $\eta=0.74$  (i.e., near random close packing).

Figure 16 shows the data for the Hg-Zn system at 250°C.  $R_{\text{core}}$  for Zn and Hg are shown in Table I. Note that at 250°C the alloy does not exist as a liquid for  $x \geq 0.6$ . The theoretical curve is computed on the assumption of a liquid throughout the concentration range with  $\eta=0.456$  at the Zn-rich end. Values of  $\eta$  are linearly interpolated between  $\eta=0.456$  and  $\eta=0.183$ .<sup>24</sup>

<sup>23</sup> G. B. Brandt and J. A. Rayne, Phys. Rev. 148, 644 (1966).

<sup>24</sup> 250°C is over twice the melting temperature (in °K) of Hg. The change in packing fraction quoted indicates a decrease in the hard-sphere diameter by about 25%. This reduction indicates an increase in penetration due to the high thermal energy of the Hg atoms. The curve of Fig. 10 is not sufficiently accurate to predict the numerical value of this decrease. In Sn, between its melting point and 1200°C, the shift in  $\eta$  required to match the resistivity requires a reduction in the hard-sphere diameter by 15%, indicating a comparably soft ion-ion interaction there as well.

The latter gives, with  $R_{\text{core}}(\text{Hg})=0.484 \text{ \AA}$ , the correct resistivity of Hg at 250°C. The over-all agreement with experiment is quite reasonable: The rapid decrease in resistivity at the Hg-rich end which appears on addition of a few percent of Zn is not well reproduced. This feature is common to a number of Hg amalgams and seems inexplicable in terms of the present model. There seems little doubt that the effect is connected with changes in properties of Hg on alloying, and probably (as we have suggested) with its potential. Note that there is a 25% change in Fermi energy in going from pure Hg to pure Zn.

A similar sharp drop in resistivity is observed in the Hg-In system. The results for this alloy are shown in Fig. 17: The experimental data are taken from Cusack *et al.*<sup>25</sup> Again we have chosen  $R_{\text{core}}(\text{Hg})=0.484 \text{ \AA}$ , and for In we have taken  $R_{\text{core}}=0.700 \text{ \AA}$ . This value fits the resistivity of the liquid just above the melting point, and the band gaps resulting from this choice give good agreement with the available low-temperature galvanomagnetic data.<sup>26</sup> It is interesting to observe that quite a large change in  $\alpha$  produces relatively little change in the initial slope of the resistivity as a function of  $x$  at the Hg-rich end.

For the Pb-Hg system, the agreement with the available potentials is not very encouraging. If we choose  $R_{\text{core}}(\text{Pb})=0.57 \text{ \AA}$ , then  $V(y)$  fits the potential of Heine and Abarenkov with some accuracy. The values at the reciprocal lattice points on the latter are

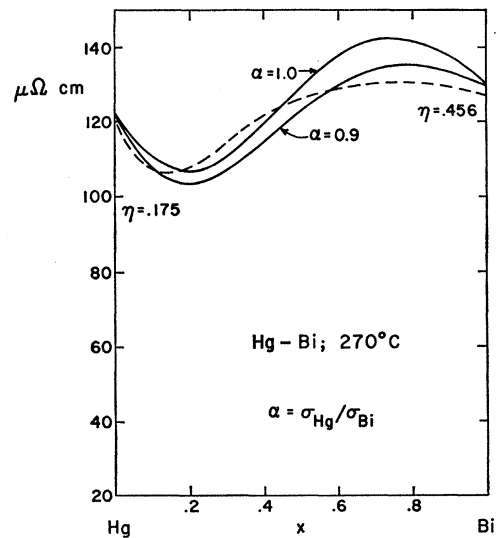


FIG. 19. Calculated resistivity of the Hg-Bi system at 270°C for two values of  $\alpha$ . The dashed experimental curve is taken from the data of Adams and Leach (private communication). The  $\eta$  value for Bi is 0.456, and for Hg is 0.175.

<sup>25</sup> N. E. Cusack, P. Kendall, and M. Fielder, Phil. Mag. 10, 871 (1964).

<sup>26</sup> N. W. Ashcroft and W. E. Lawrence (to be published). The value  $R_{\text{core}}=0.59 \text{ \AA}$  also gives fair agreement with Fermi-surface data. The resistivity results are, however, somewhat poorer than those for  $R_{\text{core}}=0.700 \text{ \AA}$ .

in good agreement with the empirical values of Anderson and Gold<sup>27</sup> which are deduced from Fermi-surface studies. As was pointed out in AL, this potential gives a resistivity of  $69.8 \mu\Omega \text{ cm}$  (compared with an experimental value of  $95 \mu\Omega \text{ cm}$ ). We have computed the resistivity of the Pb-Hg amalgam and found the discrepancy to persist throughout most of the concentration range. We have also computed the resistivity with  $R_{\text{core}}=0.78 \text{ \AA}$ . The results of both calculations are given in Fig. 18. The slight maximum observed in the experimental curve is given by the choice  $R_{\text{core}}=0.78 \text{ \AA}$  but not by  $R_{\text{core}}=0.57 \text{ \AA}$ . We comment on the  $R_{\text{core}}$  values in Sec. V.

The maximum in the resistivity-versus-concentration curve at the Pb-rich end of the Hg-Pb system is also a feature of the Hg-Bi system. The results for this alloy are obtained with the choice  $R_{\text{core}}=0.79 \text{ \AA}$  (similar to the Pb value as expected), and are given in Fig. 19.

Our remaining results concern alloys of the noble metals. Some comment is required about the potential for these metals. It is well known that the  $d$  states in Cu, Ag, and Au are of critical importance in determining their optical, cohesive, and band-structure properties for the solid phases. The anisotropy of the  $d$  bands gives rise to considerable distortions of their Fermi surfaces. Much of the anisotropy of the  $d$  states is of course linked with the structure of the unit cell, in this case the fcc system. For example, the  $d$  bands come quite close to the Fermi energy at the point  $L$ , and are partially responsible for the contact of the Fermi surface with the (111) planes. Otherwise, the Fermi surfaces in Cu, Ag, and Au are principally spherical (i.e., "s-like"). We now suggest that if the symmetry is removed (as on melting), the Fermi surfaces become essentially completely s-like. The anisotropy of the  $d$  states is smeared out by the disorder of the liquid: Their average width is of course unaffected, but the important

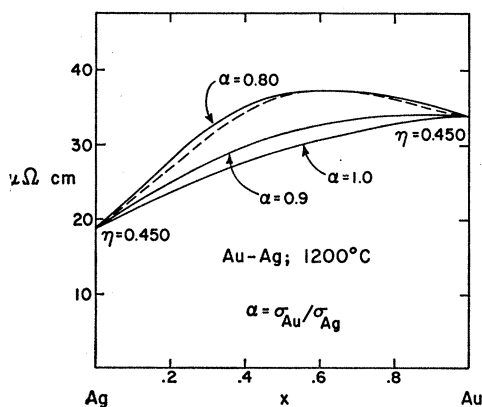


FIG. 20. Calculated resistivity of the Au-Ag system at  $1200^\circ\text{C}$  for several values of  $\alpha$ . The dashed experimental curve is taken from F. Gaibullaev and A. R. Regal, Zh. Teckhn. Fiz. 27, 2240 (1957) [English transl.: Soviet Phys.—Tech. Phys. 2, 2082 (1957)]. The  $\eta$  value was taken to be 0.45 for all  $x$ .

<sup>27</sup> J. R. Anderson and A. V. Gold, Phys. Rev. 139, A1459 (1965).

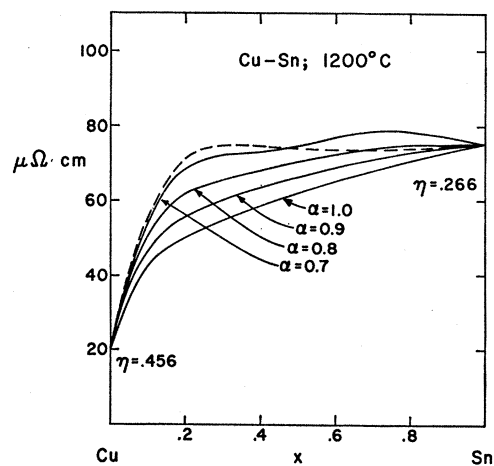


FIG. 21. Calculated resistivity of the Cu-Sn system at  $1200^\circ\text{C}$  for a number of  $\alpha$  values. The dashed experimental curve represents the data of K. Bornemann and G. Wagenmann, Ferrum 11, 276 (1913) and is cited in Ref. 1. The  $\eta$  value taken for pure Cu is 0.456 and for Sn is 0.266.

departures from the average, present in the solid, are eliminated. Thus, as regards transport, the states at the Fermi level are almost entirely s-like, the only differences from pure plane-wave behavior arising from  $s$ - $d$  overlap (which is now, however, isotropic). The latter should be small on the average, if the  $d$  system is substantially below the Fermi surface (as appears to be the case). We now find that the molten noble metals can behave as simple s-like metals and the results calculated below have been arrived at upon this assumption.

Figure 20 shows the computed resistivity for the Ag-Au system at  $1200^\circ\text{C}$ . The values of  $R_{\text{core}}$  used are given in Table I and are chosen to fit the resistivities of the pure molten metals. Again the choice is not unique but the value chosen is in agreement with the ion-ion interaction and the hard-sphere diameters estimated on the basis of a packing fraction of  $\eta=0.456$  at melting, while the other choice is not.

Finally, we have computed the resistivity of the Cu-Sn system, and the results are shown in Fig. 21. The  $R_{\text{core}}$  used for Cu is the same as the value which reproduces the ion-ion interaction shown in Fig. 9. We find reasonable agreement with data by taking  $\sigma_{\text{Cu}}/\sigma_{\text{Sn}} \sim 0.7$ . For this particular system in which there is a considerable difference in valence, we anticipate that the actual hard-core ratio will be dependent on the concentration parameter.

## V. DISCUSSION

From the agreement with experiment that we have found, we conclude that it is possible, within the simple Ziman theory, to explain quantitatively the observed resistivities of the simple binary alloys. Our calculations have required knowledge of the structure of the alloys and of the electron-ion interactions. The predominant

effect appears to be the volume dependence of the pseudopotentials rather than deviations from the modified substitutional model. Actual calculations of the ion-ion potential have enabled us to check the validity of the hard-sphere approach and, furthermore, indicate when deviations from this substitutional model are to be expected.

As regards the pseudopotentials (4) our agreement is particularly good when  $R_{\text{core}}$  is consistent with both Fermi-surface data and the resistivity of the pure liquid, and it is further known that the  $d$  states (if any) do not play an important role. In several cases there were ambiguities, which we now discuss. First, in rubidium we find the value  $R_{\text{core}}=1.12 \text{ \AA}$  to fit both the pure-liquid resistivity and the alloy data (Fig. 10) and, moreover, give good agreement with the ion-ion interaction (Fig. 7). The value  $R_{\text{core}}=1.44 \text{ \AA}$  also fits the resistivity of the pure liquid and is in fair agreement with the measured distortions on the Fermi surface.<sup>28</sup> These distortions amount to about 1%, whereas the value  $R_{\text{core}}=1.13 \text{ \AA}$  predicts less distortion, as evaluated by a simple  $s$ -electron model.<sup>26</sup> However, it is known<sup>29</sup> in Rb that the core states are not well separated in energy from the conduction band. It is quite possible, therefore, that a substantial part of the 1% distortion may be due to the anisotropy of the core states, and this effect cannot be absorbed into the simple plane-wave interpretation. The evidence on balance seems to indicate that  $R_{\text{core}}=1.12 \text{ \AA}$  is the preferred value.

For lead,  $R_{\text{core}}=0.78 \text{ \AA}$  is in agreement with the pure-liquid resistivity, alloying data (Figs. 15 and 18), and the ion-ion interaction (Fig. 12). Band gaps taken from (4) with this value of  $R_{\text{core}}$  also predict the same basic topology for the Fermi surface as observed.<sup>30</sup> The alternative value,  $R_{\text{core}}=0.59 \text{ \AA}$ , which matches the band gaps suggested by Anderson and Gold gives little agreement for all but the Fermi surface. At this point, we cannot of course discount the possibility that the spin-orbit coupling in the solid produces considerable anisotropy of the bands sufficient to alter the values of the band gaps predicted by a simple central potential of

the type (4). The latter is assumed to incorporate both central and noncentral terms and should be applicable to the liquid state where the disorder averages over any anisotropy present. We should also note that the  $d$  states in Pb are not far removed from the  $s$  band<sup>27</sup> and may also cause some slight additional distortion to the Fermi surface, not accounted for by the simple plane-wave-like expansion of the wave function.

In Cu, Ag, and Au, the  $d$  states in the free atom are fairly close in energy to the  $s$  states. Further, the usual ionic radii of singly ionized Cu, Ag, and Au are on the order of 1.0–1.3  $\text{\AA}$ ; yet for the transport potential we find values of  $R_{\text{core}}$  close to 0.5  $\text{\AA}$  for the three noble metals. These low values of  $R_{\text{core}}$  suggest strongly that the repulsive terms in the pseudopotential arise principally from the tightly bound inner core states. The repulsive part of the potential, arising from orthogonalization to  $d$  states, is relatively unimportant.<sup>31</sup> These same  $d$  states seem to be unimportant in determining the structure factor of the liquid metal, since our calculated hard-sphere radius comes well outside of the radius of the  $d$  shell. This is indicated in Fig. 9.

In summary, we find the Ziman formula for the resistivity to be quite adequate for simple binary alloys. A binary alloy is a more stringent test of the Ziman approach than a pure metal (where accidental agreement is more probable), so we regard our results as additional verification of Eq. (6) for a pure metal as well. Furthermore, by direct calculation of the interionic potential, we have confirmed the validity of the hard-sphere approach to the structure of liquid metals (at least in the region of momentum transfers important to electronic transport properties).

#### ACKNOWLEDGMENTS

We wish to thank W. Francis for the use of his Fourier-transform program and for invaluable assistance in the numerical computations. We are also very grateful to Dr. Peter Adams for helpful discussions and for access to unpublished experimental data.

<sup>28</sup> N. W. Ashcroft, Phys. Rev. **140**, A935 (1965).

<sup>29</sup> For the free atom, the core states are only about 20 eV below the  $s$  states. In lead the value is 27 eV, in Hg it is 15 eV, and in Cu it is 13 eV.

<sup>30</sup> W. E. Lawrence and N. W. Ashcroft (private communication).

<sup>31</sup> This follows because *at the Fermi surface* the overlap of a plane wave with a  $d$  state is about the same as the overlap with an inner core state, but the inner core states are much lower in energy than the  $d$  states. The small values of  $R_{\text{core}}$  are also consistent with the ionization energies of the model potential for the free atom.